害が生じることが多い[16]が，本例ではそれが明らかでなく頭頂葉病変による失読失書とはややことなる特徴を有していた．

前頭葉機能とされているワーキングメモリーに関するfunctional MRIによる検討では，言語に関しての保持と操作課題において左前頭葉前野と頭頂葉連合野の活動が上昇することが報告されており[17]，読書しても内容が理解できない，SLTAでも文章の理解が悪いといった症状は，失算の機序でも述べたワーキングメモリーの障害でも説明できる可能性がある．

左右識別障害については障害自体が軽度で持続が短かったことと発症当初に失語の合併がみられたことから，詳細に検討することができなかった．また，自分自身および検者の親指がどれか解らず，手指失認が示唆されたが，左右障害同様に詳細な検討ができなかった．しかし，WAIS-Rにおける手指パズルが完成できなかったことも手指失認症状であった可能性がある．

頭頂葉に病変をもつ「pure Gerstman's syndrome」症例の報告[7)9)]において，症候の発現機序をイメージの認知・保持・操作などの障害を中心に考察している．本症例では左前頭葉の梗塞部位以外にもSPECTで左下頭頂葉に血流低下をみとめており，前頭葉より頭頂葉にいたる経路が障害されたことによりこのイメージの障害がおこったために，不全型Gerstmann症候群および超皮質性感覚失語を呈した可能性も示唆される．

しかし，それらの報告は本例に比して明らかに手指失認・左右障害を強く呈しており，もともとの病変部位もことなっていることから，本例でとくに強かった失算や失書は前頭葉機能であるワーキングメモリー障害の関与が強いのかもしれない．

この遠隔機能障害をみとめた報告は本例以外にはなく，それらのいずれの障害を表したものであるかを決することはできない．もしくは両者の合併を表したものであり，そのために多彩な高次機能障害を呈した可能性もあると思われる．

文　献

1) 馬渕淑子，村上佰行ら：左前頭葉病変により，超皮質性感覚失語とGerstmann症候群を呈した1例．医療　1995；49：1050—1055
2) 三宅裕子，川村純一郎ら：左前頭葉脳腫瘍摘出術後にGerstmann症候群を呈した1例．失語症研究　1997；17：233—240
3) 岡崎哲也，佐伯　覚ら：左前頭葉後側にて優位半球頭頂—後頭葉の症状を認めた一例．神経心理学　2007；23：299（会識録）
4) Tohgi H, Saitoh K, Takahashi S, et al: Agraphia and acalculia after a left prefrontal (F1, F2) infarction. J Neurol Neurosurg Psychiatry 1995; 58: 629—632
5) Benton AL: The fiction of the 'Gerstmann syndrome'. J Nerurol Neurosurg Psychiatry 1961; 24: 176—181
6) 猪野正志，高山吉弘ら：失語を伴わないGerstmann症候群を呈した左視床出血の1例．臨床神経　1985；25：728—732
7) Carota A, Di Pietro M, Ptak P, et al: Defective Spatial Imagery with Pure Gerstmann's Syndrome. Eur Neurol 2004; 52: 1—6
8) Tucha O, Steup A, Smely C, et al: Toe agnosia in Gerstmann syndorome. J Nerurol Neurosurg Psychiatry 1997; 63: 399—403
9) Mayer E, Martory M, Pegna AJ, et al: A pure case of Gerstmann Syndrome with a subangular lesion. Brain 1999; 122: 1107—1120
10) 大槻美佳，相馬芳明ら：左前頭葉病変による超皮質性感覚失語の1例．脳神経　1994：46：866—871
11) Takayama Y, Sugishita M, Akiguchi I, et al: Isolated acalculia due to left parietal lesion. Arch Neurol 1994; 51: 286—291
12) Sasaki K, Tsujimoto T, Nambu A, et al: Dynamic activities of the frontal association cortex in calculating and thinking. Neuroscience Research 1994; 19: 229—233
13) Delazer M, Domahs F, Bartha L, et al: Learning complex arithmetic—an fMRI study. Brain Res Cogn Brain Res 2003; 18: 76—88
14) Gruber O, Indefrey P, Steinmetz H, et al: Dissociating neural correlates of cognitive components in mental calculation. Cereb Cortex 2001; 11: 350—359
15) McCarthy G, Puce A, Constable RT, et al: Activation of human prefrontal cortex during spatial and nonspatial working memory tasks measured by functional MRI. Cereb Cortex 1996; 6: 600—611
16) 河村　満，毛束真知子：書字の脳内メカニズム．神経進歩2003：47：755—762
17) 藤井俊勝：Working Memoryの神経機構．神経進歩2002：46：897—905

Abstract

Incomplete Gerstmann syndrome with a cerebral infarct in the left middle frontal gyrus

Yoshihito Ando, M.D.[1], Mikio Sawada, M.D.[1], Mitsuya Morita, M.D.[1], Mitsuru Kawamura, M.D.[2] and Imaharu Nakano, M.D.[1]

[1]Division of Neurology, Department of Medicine, Jichi Medical University

[2]Division of Neurology, Department of Medicine, Showa Medical University

A 65-year-old right-handed man noted a sudden onset of numbness and weakness of the right hand. On the initial visit to our hospital, he showed severe acalculia, and transient agraphia (so called incomplete Gerstmann syndrome) and transcortical sensory aphasia.

Brain MRI revealed a fresh infarct in the left middle frontal gyrus. The paragraphia and aphasia improved within 14 days after onset, but the acalculia persisted even at seven months after onset. In an ^{123}I-IMP SPECT study, the cerebral blood flow (CBF) was found to be decreased in the infarction lesion and its adjacent wide area, the ipsilateral angular and supramarginal gyri, and contralateral cerebellar hemisphere. We speculate that inactivation in the infarction lesion caused the CBF decrease in the non-infarcted areas due to diaschisis. This case indicates that Gerstmann syndrome can be caused by not only dysfunction of the angular gyrus but also of the left middle frontal gyrus in the dominant hemisphere.

(Clin Neurol, 49: 560—565, 2009)

Key words: a cerebral infarct in the left middle frontal gyrus, incomplete Gerstmann syndrome, transcortical sensory aphasia, diaschisis

Alexander 病

中野 今治（なかの いまはる） 自治医科大学教授 神経内科

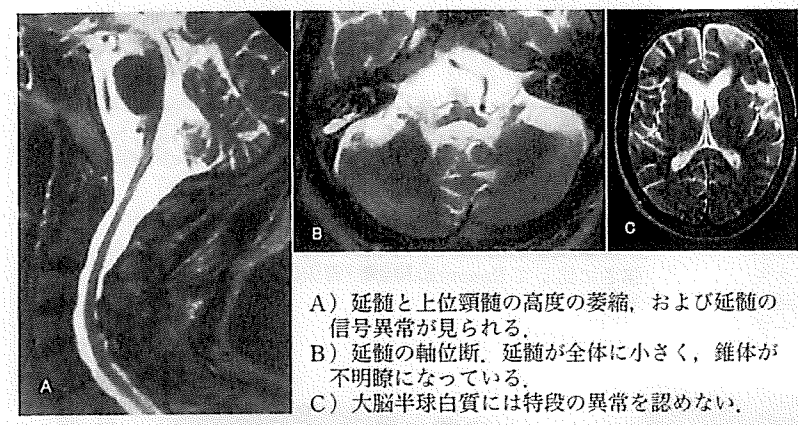

A）延髄と上位頸髄の高度の萎縮，および延髄の信号異常が見られる．
B）延髄の軸位断．延髄が全体に小さく，錐体が不明瞭になっている．
C）大脳半球白質には特段の異常を認めない．

図 1　成人型 Alexander 病 51 歳例の MRI T 2 強調画像

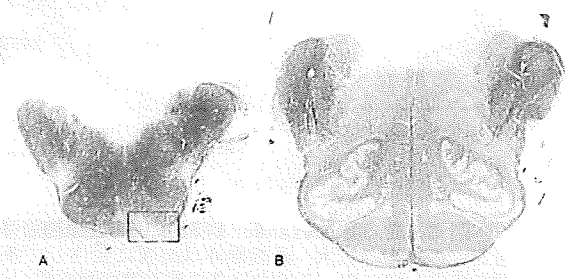

図 2　成人型 Alexander 病 51 歳例

成人型 AD(A)の延髄は対照(B)に比べて著明に小さく，錐体が変性・萎縮している．成人型 AD では下オリーブ核，延髄網様体も明らかに小さく，延髄外側部にも変性が見られる．KB．A，B はほぼ当拡大で，スケールは最小メモリが 1 mm．

Alexander 病(AD)は，神経膠線維酸性蛋白(glial fibrillary acidic protein：GFAP)の遺伝子変異を有し，星状膠細胞の細胞質内に Rosenthal 線維(RF)が出現する白質ジストロフィーである[1]*．RF は好酸性封入体で，GFAP，α-B-crystallin，熱ショックタンパク 27 を含んでいて，ユビキチン化されている．

AD には，乳児型 AD(乳児型)，若年型 AD(若年型)，成人型 AD (成人型)の三型がある．最初に報告されたのは乳児型に属する[2]．乳児型は生下時～2 歳以下で発症し，臨床的には大頭症(macrocephaly)，精神運動退行，痙縮，運動失調，痙攣を呈し，数年で死亡する[3]．病理学的には前頭葉白質の高度な変性と無数の RF の出現で特徴づけられる．若年型は 2～12 歳で発症して，進行は乳児型よりは緩徐で，協調運動障害，構音障害，嚥下障害を呈する．成人型は 10 歳台から中年，更には老年期に発症し，症候は多岐にわたるが，主として球(あるいは仮性球)麻痺症候(開鼻声を含む構音障害，嚥下障害，声帯麻痺，口蓋ミオクローヌス)，錐体路症候(下肢の痙縮，痙性歩行)，小脳性運動失調を呈する[1]．認知症は呈さない．MRI では橋のボリュームが保たれているのに対して，延髄から頸髄の高度の萎縮と MRI T 2 で髄内の高信号を呈する(図 1)(tadpole appearance)[4]．これは無症候の成人型でも見られる所見[1]であり，MRI は成人型の診断に非常に有力である．

遺伝子診断された成人型の詳細な剖検報告はごく限られている[4,5]．本稿では，われわれが経験した例[4]を中心に成人型の病理所見を述べる．

成人型で最も顕著な病理所見は，延髄から頸髄(特に延髄)が全体として非常に小さく，延髄錐体が高度に侵されていることである(図 2)．錐体は強い粗造化を呈し，多数の小空胞がそれぞれ独立に，あるいは癒合して認められる．不思議なことにその中を貫通している舌下神経の髄内根は保持されている(図 3)(本例では舌萎縮は見られなかった)．また，延髄錐体では，組織荒廃が強いのに対して RF の数は驚くほど少ない(図 4)．

延髄は変性箇所のみでなく全体に作りが小さく，グリオーシスも明らかではない．下オリーブ核は対照に比べてその幅が狭く，また，ニューロンの密度も高い(図 5 A，B)．そのニューロピルは良く保たれ，明らかなグリオーシスは見られず，変性により萎縮したとは考えにくい．神経核内のニューロン間の距離を決めるのはその突起，特に樹状突起の発達状態であることと，変性所見が見られないことを考えると，下オリーブ核には発達障害の存在が推測される．延髄全体が小さいのも形成不全の可能性がある．

頸髄も全体に小さいが，最も目立つのは延髄錐体の変性・壊死に符合する錐体側索路の変性である(図 6)．

橋以上の脳幹，大脳には特段の変性像は見られない(図 7)．RF は脳室に接した白質(脳梁下層 stratum subcallosum，半輪状条 stria semicircularis，海馬采 fimbria hippocampi)に少数見られるのみ(図 7)であり，大脳脳溝深部の軟膜下組織に中等数認められる(図 8)．

AD に関して MRI 所見と剖検所見を併せて考えると，① 病巣は，乳児型では大脳の広範な領域に及ぶのに対して，若年型では脳幹に移動する傾向を示し，成人型ではさらに下がって延髄と頸髄に限局する，② RF は乳児型，若年型，成人型と発症年齢が高くなるにつれて少なくなる傾向が見られる，とまとめることができる．

*典型的な成人型 AD で GFAP 遺伝子変異を伴わない症例が少数報告されており，本症は遺伝的に不均一であり，GFAP 以外の遺伝子異常が存在する可能性がある(http://www.waisman.wisc.edu/alexander/を参照されたし)．また，重篤な内科疾患を有する成人患者で脳に多数の RF が出現する症例[6]が知られているが，これは成人型 AD には含めないことにする．

文　献

1) Pareyson D, Fancellu R, Mariotti C, et al. Adult-onset Alexander disease : a series of eleven unrelated cases with review of the literature. Brain. 2008 ; 131 : 2321.
2) Alexander WS. Progressive fibrinoid degeneration of fibrillary astrocytes associated with mental retardation in a hydrocephalic infant. Brain. 1949 ; 72 : 373.
3) Li R, Johnson AB, Salomons G, et al. Glial fibrillary acidic protein mutations in infantile, juvenile, and adult forms of Alexander disease. Ann Neurol. 2005 ; 57 : 310.
4) Namekawa M, Takiyama Y, Aoki Y, et al. Identification of GFAP gene mutation in hereditary adult-onset Alexander's disease. Ann Neurol. 2002 ; 52 : 779.
5) Stumpf E, Mason E, Duquette A, et al. Adult Alexander disease with autosomal dominant transmission. A distinct entity caused by mutation in the glial fibrillary acid protein gene. Arch Neurol. 2003 ; 60 : 1307.
6) Riggs JE, Schochet SS Jr, Nelson J. Asymptomatic adult Alexander's disease : entity or nosological misconception ? Neurology. 1988 ; 38 : 152.

0289-0585/09/￥500/論文/JCOPY

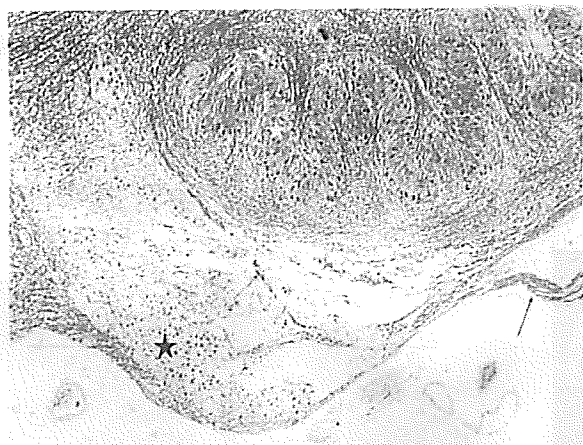

図 3　成人型 Alexander 病 51 歳例の左延髄錐体
図 2 A の枠内の拡大．延髄錐体は高度に変性して多数の小空洞を形成している．その中を走る舌下神経髄内根(ピンク矢印)と髄外根(赤矢印)は保たれている．また，壊死は錐体路にほぼ限局しており，壊死部に接する弓状核(赤★)と下オリーブ核(黄★)は保たれている．KB，×40.

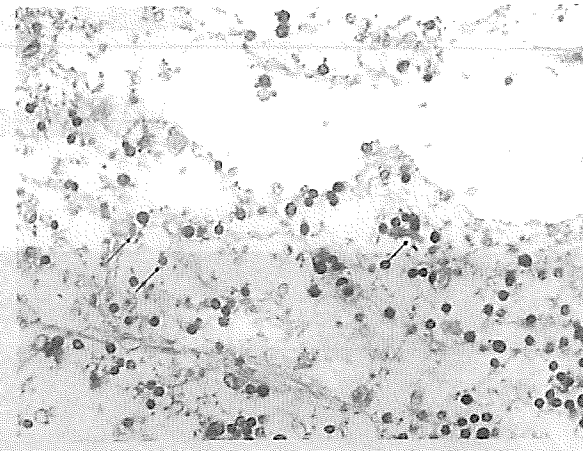

図 4　成人型 Alexander 病 51 歳例の左延髄錐体
錐体は高度に荒廃し，小空洞を形成している．変性の強さに比して Rosenthal 線維(青矢印)は少ない．HE，×400.

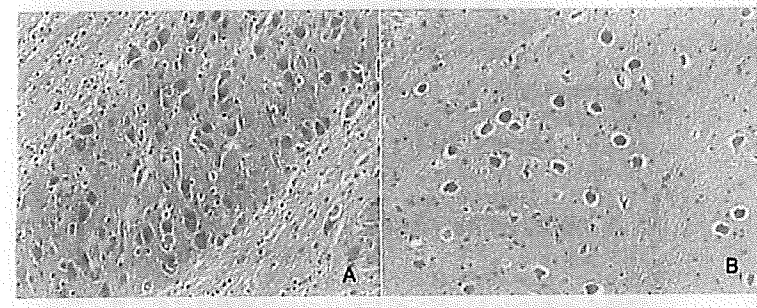

図 5　成人型 Alexander 病 51 歳例
下オリーブ核(A)のニューロン密度は対照(B)に比して明らかに高い(ニューロン間の距離が小さい)．また，成人型 AD 例下オリーブ核のニューロピルは密でグリオーシスも見られない．HE，×200.

図 6　成人型 Alexander 病 51 歳例．第 7 頸髄
錐体側索路，錐体前索路とも延髄錐体の変性に応じた変性を示している．前角の萎縮や前角大型ニューロンの脱落はない．KB，×6.

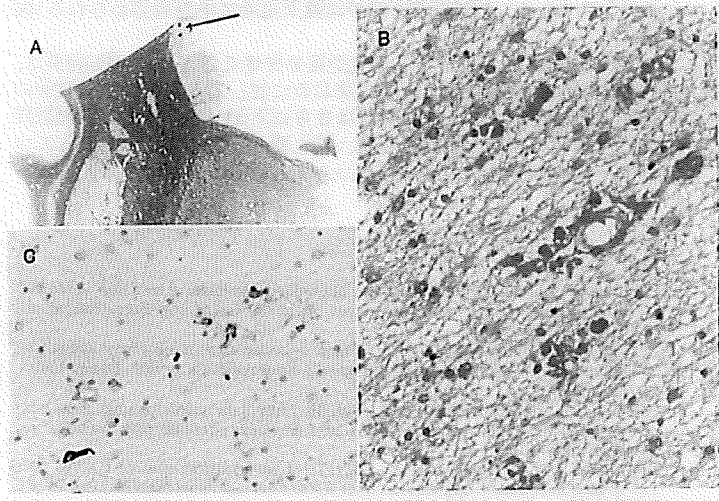

図 7　成人型 Alexander 病 51 歳例の脳梁下層(stratum subcallosum)
A) 赤矢印が脳梁下層．放線冠や内包の白質に変性は見られない．KB，×5. B) 脳梁下層には少数の Rosenthal 線維が見られる．HE，×400. C) Rosenthal 線維は辺縁がより強く染まる．抗ユビキチン抗体免疫染色，×400.

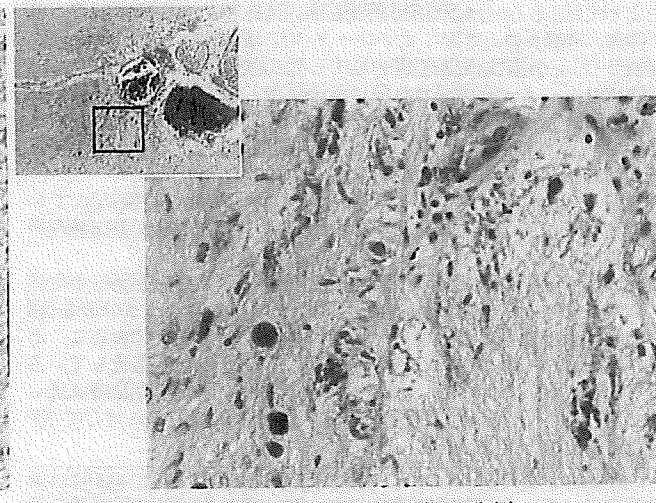

図 8　成人型 Alexander 病 51 歳例
大脳皮質の脳溝深部の軟膜下層(左上)．本例で Rosenthal 線維が最も多く見られる箇所である(右下：左上の枠の拡大)．HE，左上×10，右下×400.

日本で初めての パーキンソン病遺伝子治療

自治医科大学　教授（医学部内科学講座　神経内科学部門）
中野（なかの）　今治（いまはる）

パーキンソン病と現在の治療法

パーキンソン病は、40～70歳で発病する脳の病気で、振戦（ふるえ）、寡動（動作が少なく、かつ遅い）、筋強剛（体が硬い）、姿勢反射障害（転びやすい）が主な症状です。通常は発病後７～８年で寝たきりとなりますが、その期間は３～15年とかなりの幅があります。

脳の中脳と呼ばれるところに黒質という場所があります。黒質の神経細胞はドパミンを作り出す細胞（ドパミン合成細胞）で、線条体というところに突起（軸索）を伸ばし（図１，２）、この突起の先端でドパミンが作られて線条体で放出されます。健常人では、ドパミン合成の第一段階として、本来ドパミン合成細胞の中に在るチロシンから、チロシン水酸化酵素（TH）の働きによってレボドパが合成されます。このレボドパが芳香族Ｌアミノ酸脱炭酸酵素（AADC）によってドパミンに変換され、線条体で放出されて、線条体の神経細胞に作用するという仕組みになっています（図２）。ドパミンを受け取った線条体の神経細胞の一部は、最終的に視床下核という構造の神経細胞を抑制して運動が滑らかに行われるようにしています。

パーキンソン病では、この黒質のドパミン合成細

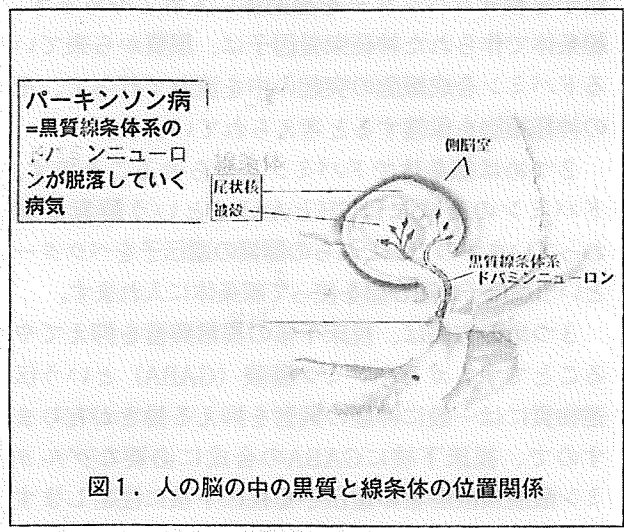

図１．人の脳の中の黒質と線条体の位置関係

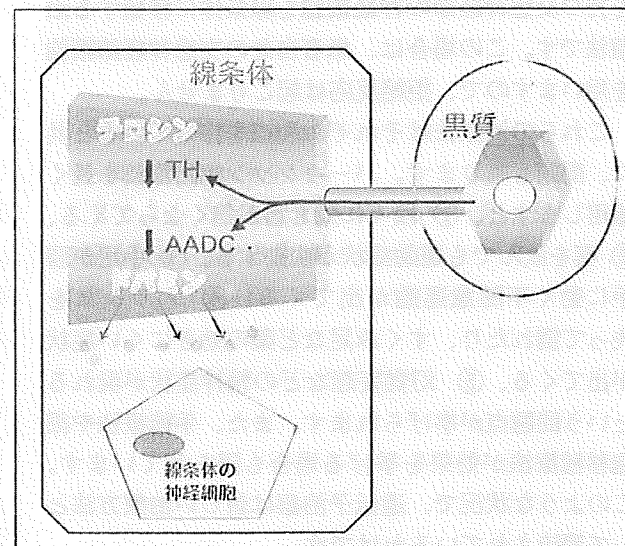

図２．健常人のドパミン合成細胞と線条体．
黒質に在るドパミン合成細胞は、線条体に突起を送り、そこでドパミンを合成して線条体に放出する．ドパミンは線条体に在る神経細胞に働く．
TH：チロシン水酸化酵素、AADC：芳香族アミノ酸脱炭酸酵素．

胞が徐々に死んで行きます。そのために線条体のドパミンが足りなくなることで発病すると考えられています（図3）。線条体でドパミンが足りなくなりますと、上に述べた視床下核の神経細胞が異常に興奮し、このことが症状の出現に関係しています。私たちが行っている遺伝子治療と関係して大切なことは、パーキンソン病ではドパミンを合成する黒質の細胞は死ぬのに対して、ドパミンを受け取る線条体の神経細胞は死なないと言うことです。このことがここで述べるパーキンソン病の遺伝子治療に対する戦略の要となります。

現在、パーキンソン病治療の原則は薬物療法です。その中心となるのはドパミンの前段階の物質（前駆物質）であるレボドパです。そのほかにドパミンと類似の働きをするドパミン作動薬、放出されたドパミンの分解を防ぐモノアミン酸化酵素阻害薬、ドパミンと拮抗するアセチルコリンの作用を抑える抗コリン薬、ドパミンの放出を促すアマンタジンがあります。そして、服用したレボドパが脳に入る前に分解されるのを防ぐCOMT阻害薬（エンタカポン）も開発されました。

薬以外の治療としては、手術療法や細胞移植療法があります。手術療法の主体は深部脳刺激ですが、視床破壊術や淡蒼球破壊術なども行われます。また、細胞移植は、黒質のドパミン合成細胞と類似の働きを持つ交感神経節の神経細胞を線条体に移植する治療法です。この場合は、患者自身の交感神経節細胞を用いますので、拒絶反応は起こりません。

これらの治療法はそれぞれ利点を持っていると共に、問題も有ります。パーキンソン病治療薬を長く服用しますと、① 段々に効き目が無くなってくる、② 薬を飲んでも運動症状が変動する、③ 手足が勝手に動く不随意運動が出てくる、④ バランスを失って倒れたり、すくみ足など薬の効きにくい症状が出てくる、⑤ 幻覚妄想などの精神症状が現れるという問題点が挙げられます。また、手術療法や細胞移植療法が効果を挙げる場合も限られています。このような状況で、遺伝子治療は新しい治療方法として期待されているわけです。

ここではパーキンソン病の遺伝子治療について、私たちが今回実施した方法を中心にして述べることにします。

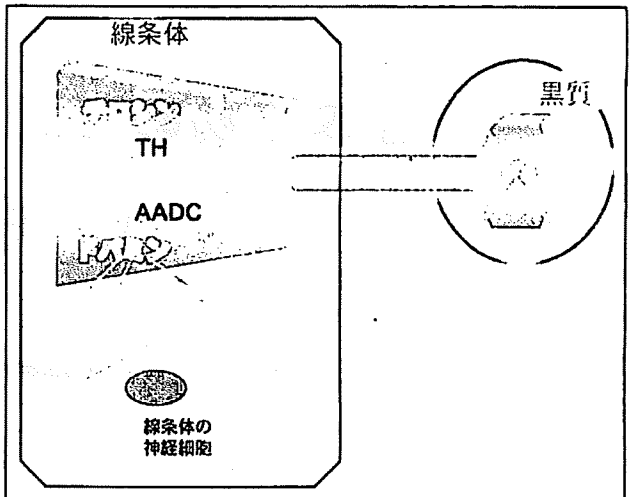

図3　パーキンソン病のドパミン合成細胞と線条体．パーキンソン病では黒質のドパミン合成細胞が死ぬために線条体でドパミンが不足する．線条体の神経細胞は生きのびている．TH：チロシン水酸化酵素、AADC：芳香族アミノ酸脱炭酸酵素．

パーキンソン病の遺伝子治療戦略

上に触れましたように、パーキンソン病発病の主なメカニズムは、① 黒質のドパミン合成細胞が脱落して、② 線条体でドパミンが足りなくなり、③ その結果、視床下核が異常に興奮した状態になることに有ると考えられます。従って、パーキンソン病の遺伝子治療の方法としては、それぞれのメカニズムを抑えることを目指した3つの方法が考えられます。

1つめは黒質のドパミン合成細胞が死ぬのを防いでやることです。この場合には、この細胞の保護作用を持っている神経栄養因子というタンパク質の遺伝子を載せたベクターを線条体に入れてやります。線条体で作られた神経栄養因子は、黒質から来ているドパミン合成細胞の突起の中を流れて行って、その神経細胞を保護すると考えられています。

2つめは線条体でドパミンを作らせることです。ドパミンの合成にはTHとAADCという酵素が関わっていますので、これらの酵素の遺伝子をベクターという遺伝子の運び屋を使って線条体に入れます。

3つめの方法は、視床下核の異常興奮を抑えてやることです。ガンマアミノ酪酸（GABA）という伝達物質には一般に神経の興奮を抑える働きが有りますので、視床下核にGABAの合成に必要なグルタミン酸脱炭酸酵素の遺伝子を視床下核に注射します

と、GABAが作られてそこの異常興奮を抑えることができます。３つの方法とも定位脳手術により、目的とする場所に遺伝子を載せたウイルスを注射します。

アデノ随伴ウイルス(AAV)をベクターとして使用

ベクターとは、治療用に使う遺伝子の運び屋です。ベクターにはいくつか種類がありますが、ウイルスベクターはこの運び屋としてウイルスを使った場合の名称です。

アデノ随伴ウイルス（AAV）は自然界に存在するありふれたウイルスのひとつで、多くの人が気づかないうちに感染しています。このウイルスはそれ自身では増えることができず、人の病気も起こしません。ウイルス由来のタンパク質の遺伝子を取り外して、空いた部分に治療用の遺伝子を載せたものが治療用ベクターです。私たちの遺伝子治療では、この空いた部分にAADCの遺伝子を入れてあります（図４）。

パーキンソン病に対する私たちの遺伝子治療の考え方

自治医大の遺伝子治療研究グループ（神経内科、遺伝子治療研究部、脳神経外科）は、パーキンソン病のモデルサルで遺伝子治療実験を行って、安全で効果が有ることを確認した後に、人での治療研究の計画を立てました。

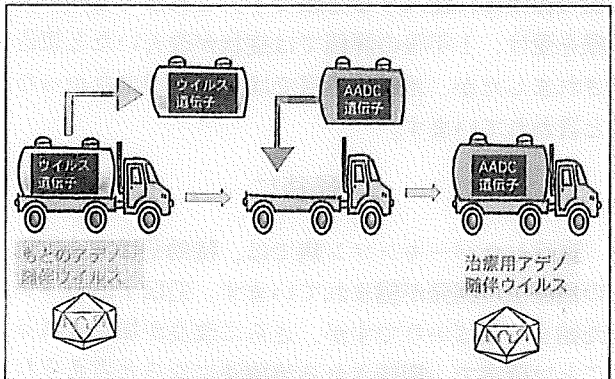

図４．治療用ベクターの構造の模式図.
自然界のアデノ随伴ウィルスは、荷台にウィルスのタンパク質を合成する遺伝子を積んだトラックにたとえられる．この遺伝子を取り除いて、ドパミンを合成する酵素の遺伝子（AADC）に積み替えたトラックが治療用ベクターである．

サルの研究では、ドパミン合成に必要なチロシン水酸化酵素（TH）、GTPシクロヒドラーゼⅠ（GCH）、芳香族Lアミノ酸脱炭酸酵素（AADC）の遺伝子を線条体に注射しました（図５）。しかしながら、人に３種類の遺伝子を最初から注射するのは安全性の点で問題があります。そこで、まずAADCの遺伝子のみ線条体に注射することにしました。

AADCの遺伝子を線条体に入れて、そこの神経細胞でAADCを作ります。そうしておいてレボドパをのみますと、レボドパがその細胞の中に入って、この酵素によってドパミンに変わり、線条体に放出されます（図６，７）。作られるドパミンが多すぎると副作用が出る恐れがあります。しかし、この方法ですと、万一AADCが大量に作られすぎたとしても、服用するレボドパを減らせば作られるドパミンの量も減りますので、副作用の心配もなくなります。AADCは言わばドパミンを作る工場であり、レボドパがその原料、ドパミンが製品に相当します。工場が多く建てられすぎても材料が少なければ製品は少ししかできないのと同じ原理です。

この計画に基づいて、パーキンソン病のモデルサルでも人で行うのと同じ方法を試してみました。その結果、AADCの遺伝子だけの注射（工場を作るだけ）では効果が無いこと、そのサルにレボドパをのませること（工場に原料を供給する）で初めてドパミン（製品）が作られて効果が現れ、サルの動きが

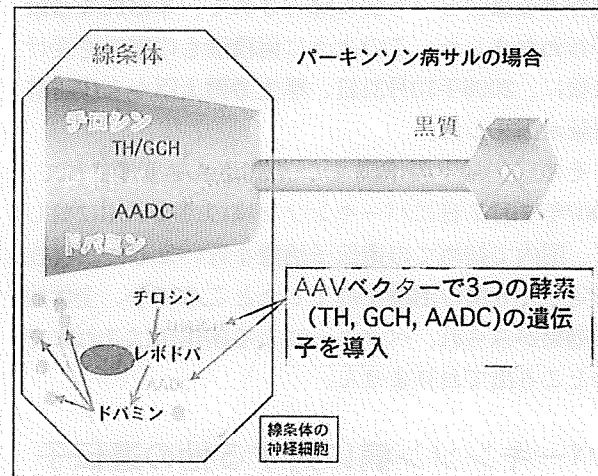

図５．パーキンソン病のモデルサルでの遺伝子治療実験.
サルの場合には３つの酵素（TH：チロシン水酸化酵素、GCH：GTPシクロヒドラーゼ Ⅰ、AADC：芳香族アミノ酸脱炭酸酵素）の遺伝子を同時に入れて安全で効果が有ることを確認した．

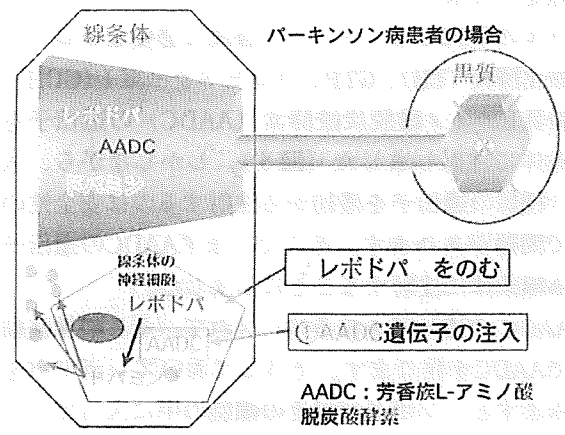

図6．パーキンソン病の遺伝子治療の第一段階．AADCの遺伝子のみを線条体に注射し、レボドパをのんでドパミンを作らせる．

良くなることが確認されました。

パーキンソン病に対する私たちの遺伝子治療の実施

以上のような考え方に立って、進行したパーキンソン病を対象とした遺伝子治療計画を作り、まず、自治医科大学附属病院遺伝子治療臨床研究審査委員会に提出して、十分な審査を受けました。そこで研究計画が認められた後に、今度は厚生労働省の厚生科学審議会科学技術部会に計画書を申請し、そこでの審議を経た後にパーキンソン病遺伝子治療臨床研究作業委員会という会に降ろされて、本格的な審議が行われました。このように何段階もの審査を受けた後に、2006年10月31日、厚生労働大臣から実施許可証が出ました。

その後、様々の準備をし、患者さんも募集して、2007年5月7日にパーキンソン病の患者さんに対して、国内で初めての遺伝子治療を行いました。現在予定した6例の治療を終了したところです。全体的に効果がみられ、ベクターによる副作用はこれまでのところ出ておりません。

パーキンソン病に対する他の遺伝子治療法

先に、パーキンソン病に対する遺伝子治療の考え方には大きく3つ有ることを述べました。私たち以外に、パーキンソン病の遺伝子治療が実際に行われ

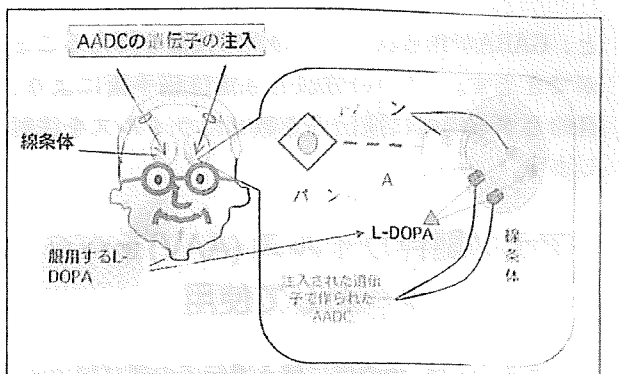

図7．パーキンソン病遺伝子治療の模式図2．

ているのはアメリカのみで、先に触れた3つの方法が行われています。3つの遺伝子治療ともベクターとしてアデノ随伴ウイルスを用いています　注入はいずれも定位脳手術で行っています。

私たちと同じ方法で行っているのは、カリフォルニア大学サンフランシスコ医療センターで、ここでは既に9例の治療が行われています。

もう一つの治療では、視床下核の異常興奮を抑えるために片側にのみグルタミン酸脱炭酸酵素（GAD）の遺伝子を注射します。この方法は、2003年にコーネル大学で開始され、現在最初の12例が終了してイギリスの医学雑誌ランセットに論文が発表されました。それによりますと、治療側の手足（注射と反対側の手足）で1年後でも症状の改善が認められ、PETを使って遺伝子の働きが確認されたとのことです。

3番目の治療法は、神経栄養因子の一つであるニュールトリン（NTN）という物質の遺伝子を両側の線条体に注入する方法です。これまで12例が治療を受け、1年後の評価では症状が改善したと報告されましたが、治験第Ⅱ相では有意差が出なかったと言われています。

最後に

進行したパーキンソン病では、特効薬はなく新規の治療法の開発が望まれています。遺伝子治療はまだ始まったばかりですが、さらに改良が加えられることは確実で、期待される治療法になると考えられます。

Aberrant promoter methylation and expression of the imprinted *PEG3* gene in glioma

By Susumu OTSUKA[*1,*2], Shinji MAEGAWA[*1], Ayumi TAKAMURA[*1], Hideki KAMITANI[*3], Takashi WATANABE[*3], Mitsuo OSHIMURA[*2] and Eiji NANBA[*1,†]

(Communicated by Takao SEKIYA, M.J.A.)

Abstract: Glioma includes astrocytoma, oligodendroglioma, ependymoma and glioblastoma. We previously reported the epigenetic silencing of paternally expressed gene 3 (*PEG3*) in glioma cell lines. In this study, we investigated methylation of an exonic CpG island in the promoter region and the expression of *PEG3* gene in 20 glioma and 5 non-tumor tissue samples. We found wide variations in the methylation level. Hypomethylaiton and hypermethylation was found in 3 and 4 glioma tissue samples, respectively. Monoallelic expression, which is an evidence of an imprinted gene, was maintained in eight out of nine informative cases which have T/C polymorphisms in *PEG3*. The lower gene expression, which suggested epigenetic silencing of *PEG3*, was confirmed statistically in glioblastoma using quantitative reverse-transcription polymerase chain reaction. Interestingly, we found higher expression of *PEG3* in two out of three oligodendrogliomas. A negative correlation between the methylation level and gene expression was shown by regression analysis. These results suggest that the abnormal regulation of *PEG3* is associated with several glioma subtypes and that it plays an important role in tumorigenesis.

Keywords: glioma, *PEG3*, DNA methylation, epigenetic silencing

Introduction

Paternally expressed gene 3 (*PEG3*) is an imprinted gene located on 19q13.4. *PEG3* encodes a krüppel-type (C2H2) zinc-finger protein and is expressed predominantly in brain, ovary, testis and placenta in adult tissues.[1] Although its function has not been completely characterized, *PEG3* has been reported to play an important role in cell proliferation by activating NF-κB[2] and in p53-mediated apoptosis by inducing Bcl2-associated X protein (Bax) translocation.[3)–5] In female mice lacking *Peg3*, which is mouse homologue of human *PEG3* gene,[6] growth impairment and compromised nurturing behavior have been seen, although glioma genesis has not been reported.[7)–9] *PEG3* is believed to be involved in the development of various brain regions, such as the hypothalamus, through its role in apoptotic pathways.

Tumor suppressor activity of the human *PEG3* gene has been reported in human glioma cell lines.[10] In a previous study, we reported that the aberrant DNA methylation of the CpG island is associated with epigenetic silencing of *PEG3* in glioma cell lines.[11] We also identified a novel imprinted transcript gene called *ITUP1*, which is located upstream and oppositely oriented to *PEG3* and is expressed on the paternal chromosome. The expression profile of *ITUP1* was similar to that of *PEG3* in glioma cell lines[12] suggested methylation status of the CpG island is important for regulation of these genes.

To date, however, there are a few studies about *PEG3* gene in tumor tissues of glioma. These studies are about oligodendroglioma.[10),26)] Therefore, relationship between *PEG3* gene and other

[*1] Division of Functional Genomics, Research Center for Bioscience and Technology, Tottori University, Tottori, Japan.
[*2] Department of Biomedical Science, Regenerative Medicine and Biofunction, Graduate School of Medical Science, Tottori University, Tottori, Japan.
[*3] Department of Neurosurgery, Institute of Neurological Science, Tottori University, Tottori, Japan.
[†] Correspondence should be addressed: E. Nanba, Division of Functional Genomics, Research Center for Bioscience and Technology, Tottori University, 86 Nishicho, Yonago, Tottori 683-8503, Japan (e-mail: enanba@med.tottori-u.ac.jp).

Abbreviations: *PEG3*: paternally expressed gene 3; *GAPDH*: glyceraldehyde-3-phosphatase dehydrogenase; PCR: polymerase chain reaction; qRT-PCR: quantitative reverse transcription PCR; MSP: methylation-specific PCR; ML: methylation level; ANOVA: analysis of variance.

doi: 10.2183/pjab/85.157

Table 1. Expression data for *PEG3* in non-tumor and glioma brain samples

Sample	Sex	Age	Diagnosis	WHO grade	Genotype	Expression
GT18	M	11	dysembryoplastic neuroepithelial tumor	I	C/C	+
GT2	F	6	Astrocytoma	II	C/T	+ (C)
GT15	F	34	Astrocytoma	II	C/T	+ (T)
GT13	M	3	Ependymoma	II	C/T	+ (C)
GT4	M	22	Ependymoma	II	C/C	+
GT16[d]	M	32	Oligodendroglioma	II	C/T	+ (T)
GT12	M	43	Anaplastic Astrocytoma	III	C/T	+ (T)
GT20[b]	M	70	Anaplastic Astrocytoma	III	C/T	+ (C)
GT10	F	11	Anaplastic Ependymoma	III	C/T	+ (T)
GT14	F	51	Anaplastic Oligodendroglioma	III	T/T	+
GT7	M	45	Anaplastic Oligodendroglioma	III	T/T	+
GT5	F	35	Glioblastoma	IV	C/T	+ (T)
GT11[a]	F	39	Glioblastoma	IV	T/T	+
GT6	F	71	Glioblastoma	IV	T/T	+
GT17	M	17	Glioblastoma	IV	T/T	+
GT19	M	25	Glioblastoma	IV	C/C	+
GT3[c]	M	35	Glioblastoma	IV	C/T	ND
GT1	M	66	Glioblastoma	IV	T/T	+
GT9	M	66	Glioblastoma	IV	C/C	+
GT8	M	70	Glioblastoma	IV	T/T	+
B16[a]	F	39	Non-tumor	—	T/T	+
B15	F	49	Non-tumor	—	C/T	+ (T)
B19[d]	M	32	Non-tumor	—	C/T	+ (T)
B18[c]	M	35	Non-tumor	—	C/T	+ (T)
B17[b]	M	70	Non-tumor	—	C/T	+ (C)

F: female; M: male; ND: not determined, were indicated. a–d: the same alphabet means the same person respectively.

subtypes and malignancy grades of glioma is not clear. In this study, we examined the methylation and expression of *PEG3* in glioma tissues to evaluate its availability of diagnosis and treatment of this tumor.

Materials and methods

Brain tissues. Samples of 20 gliomas (samples GT1–GT20) and 5 non-tumor brain tissues (samples B15–B19) were obtained from Tottori University Hospital, Yonago, Japan. They included 8 female and 13 male patients who ranged in age from 3 to 71 years. The study was approved by the Ethical Committee of the Faculty of Medicine, Tottori University, and informed consent was obtained from all patients.

Tumor samples were classified by a surgical pathologist using the World Health Organization (WHO) system.[13] We found one sample of grade I (dysembryoplastic neuroepithelial tumor), 5 samples of grade II (2 astrocytomas, 2 ependymomas and 1 oligodendroglioma), 5 samples of grade III (2 anaplastic astrocytomas, 1 anaplastic ependymoma and 2 anaplastic oligodendrogliomas) and 9 samples of grade IV (9 glioblastomas) (Table 1). For this study, we unified the samples of grade I and II tumors into the "low grade" category. Non-tumor brain was obtained as normal control. Four of the five non-tumor brain samples B16, B17, B18 and B19 adjacent to the tumor were obtained from the patients with glioma GT11, GT20, GT3 and GT16, respectively. B15 was obtained from a patient of brain ischemia. All samples were snap frozen in liquid nitrogen and stored at −80 °C before the extraction of DNA or RNA.

Extraction of nucleic acids and cDNA synthesis. Genomic DNA was extracted using standard phenol-chloroform extraction. Total RNA was extracted by using the RNeasy mini kit (QIAGEN, Hilden, Germany) according to the manufacturer's

instructions and then treated with DNase I (Nippon Gene, Tokyo, Japan) to remove DNA. To investigate the possibility of DNA contamination, the first-strand cDNA was synthesized with (RT+) or without (RT-) M-MLV reverse transcriptase (Invitrogen, Carlsbad, CA, USA) using random primers (Promega, Madison, WI, USA). Reaction conditions were 25 °C for 10 min, 42 °C for 50 min and 95 °C for 5 min. To confirm the synthesis of first-strand cDNA, the expression of human glyceraldehyde-3-phosphatase dehydrogenase (*GAPDH*) was detected using polymerase chain reaction (PCR) primers qGAPDH forward (5′-TGAACGGGAAGCTCACTGG-3′) and qGAPDH reverse (5′-TCCACCACCCTGTTGCTGTA-3′). The PCR conditions were 30 cycles of 95 °C for 30 s, 55 °C for 30 s and 72 °C for 30 s.

Bisulfite treatment of genomic DNA and DNA methylation analysis. Extracted genomic DNA from tumor and non-tumor samples was treated with sodium bisulfite as previously described.[14] Bisulfite treated genomic DNA-sequencing was then performed as previously described.[12] For each DNA sample, ten clones were analyzed. We examined a total of 33 CpG sites in the CpG island. The sequencing was performed from both directions using the BigDye Terminator v3.1 cycle sequencing kit and ABI3130xl genetic analyzer (Applied Biosystems, Foster City, CA, USA).

Methylation-specific PCR (MSP) assay. *PEG3* is an imprinted gene and has both unmethylated and methylated alleles normally. Thus it is necessary to gauge ratio of both alleles to assess epigenetic difference. To measure relative methylated level, we performed MSP with assessable trait as below. Two sets of primers (U and M) designed for annealing to bisulfite-modified genomic DNA were used in this experiment. One primer set (U) annealed to unmethylated DNA that had undergone chemical modification. A second set (M) annealed to methylated DNA that had undergone chemical modification. Primer sets used for MSP were previously described[11] (Fig. 1). For equalizing intensities of unmethylated and methylated bands in non-tumor brain tissues, the PCR conditions were set as follows: for unmethylated DNA, 35 cycles of 95 °C for 1 min, 60 °C for 1 min and 72 °C for 1 min; and for methylated DNA, 34 cycles of 95 °C for 1 min, 62 °C for 1 min and 72 °C for 1 min. PCR products were resolved in 2% agarose gel and visualized by ethidium bromide staining. Intensities of the U and M bands were analyzed using Densitograph version 4.0 software (ATTO, Tokyo, Japan) to measure band ratio of MSP.[15]

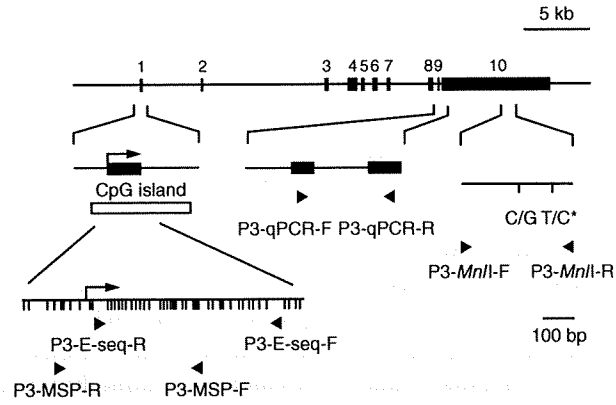

Fig. 1. A schematic map of *PEG3* gene.
Exons are indicated by black boxes. Numbering is followed by the information of GenBank accession no. AC006115. A CpG island surrounding exon 1 (open box), which is the transcriptional starting site of *PEG3* (arrow), was identified by the ORNL GRAIL Form. Detailed CpG sites are indicated in lower left panel. DNA methylation was investigated by bisulfite genomic sequencing and MSP by using PCR primers designed on the CpG island indicated by arrowheads.[11),12)] Quantitative PCR analysis was performed with the primers P3-qPCR-F and P3-qPCR-R (arrowheads) designed on exon 9 and 10, respectively. Primer sequences are described in materials and methods. Imprinting test was performed with the primers P3-*Mnl*I-F and P3-*Mnl*I-R (arrowheads).[11)] Single nucleotide polymorphisms (SNPs) are shown as sequence polymorphism. The SNP analyzed for allelic expression (asterisk) is located at position 134718 on AC006115.

Genomic imprinting test. To distinguish parental alleles, we performed direct sequencing analysis to find T/C polymorphisms in exon ten of *PEG3*. DNA and cDNA from tumor and non-tumor brain tissue samples were amplified using PCR primers previously described[11] (Fig. 1).

Quantitative gene-expression analysis. For quantitative reverse-transcription PCR (qRT-PCR), we used LightCycler fast-start DNA SYBR green I (Roche, Basel, Switzerland) and a LightCycler Real-Time PCR system (Roche). We used the primers P3-qPCR forward (5′-CAAGAGAAGTGCCTACCCA-3′) and P3-qPCR reverse (5′-GAACTGCGTGACACATCC-3′) for *PEG3* (Fig. 1) with the following PCR conditions: 45 cycles of 95 °C for 15 s, 60 °C for 5 s and 72 °C for 6 s. As an internal standard, *GAPDH* was detected with PCR primers qGAPDH forward and reverse. The PCR

conditions were 45 cycles of 95 °C for 15 s, 55 °C for 5 s and 72 °C for 10 s. PCR products were resolved in 2% agarose gel and visualized by ethidium bromide staining. Gene-specific standard curves were generated using 10-fold serial dilutions of plasmid DNAs of a 147-bp *PEG3* clone and a 307-bp *GAPDH* clone.

Data analysis. Data of MSP were pooled from three independent sets of experiments, and we calculated the methylation level (ML) using the following formula: methylated band/(intensity of methylated band + intensity of unmethylated band). An ML > 0.60 was defined as hypermethylation and an ML < 0.40 was defined as hypomethylation. Means ± 2 S.D. of the MLs of non-tumor brain tissues (except for sample B19) were included in these definitions. Data of qRT-PCR were pooled from three independent sets of experiments. These data were analyzed by one-way analysis of variance (ANOVA), Student's *t* test and regression analysis.

Results

Methylation of the exonic CpG island in *PEG3*. To determine the methylation level, we performed MSP. At first, we tested on non-tumor brain tissues. Approximately equivalent florescence intensities were detected from the U and M bands in four out of five non-tumor brain tissues (Fig. 2A). We performed this experiment three times and obtained similar results. Thus, MLs were calculated from the values of U and M band intensity as described in Materials and Methods. ML values in non-tumor brain tissues ranged from 0.48 to 0.52, except for that of sample B19. Then, we tested in glioma tissue samples (Fig. 2A). We detected both U and M bands from every sample in three sets of experiment. In samples GT18, GT4 and GT9, ML values were 0.58, 0.47 and 0.52, respectively. This implied methylation levels in these tumor samples were same as non-tumors. ML values in 13 out of 20 tumors were indicated normal range. On the other hand, we found wide variations in other tumor tissues. In samples GT2 and GT7, the U band was predominant and ML values were 0.33 and 0.14, respectively. These results implied that the CpG island was hypomethylated in these samples. In samples GT8, GT20 and GT17, the M band was predominant and MLs were 0.92, 0.65 and 0.68, respectively. These results implied hypermethylation of the CpG island. Finally, three samples indicated hypo- and four samples did hypermeth ylation. To confirm the MSP results, we performed bisulfite sequencing on all tissue samples (Fig. 2B). Although there was slight difference with fraction of clone number in each sample, the results were approximately consistent with those of MSP.

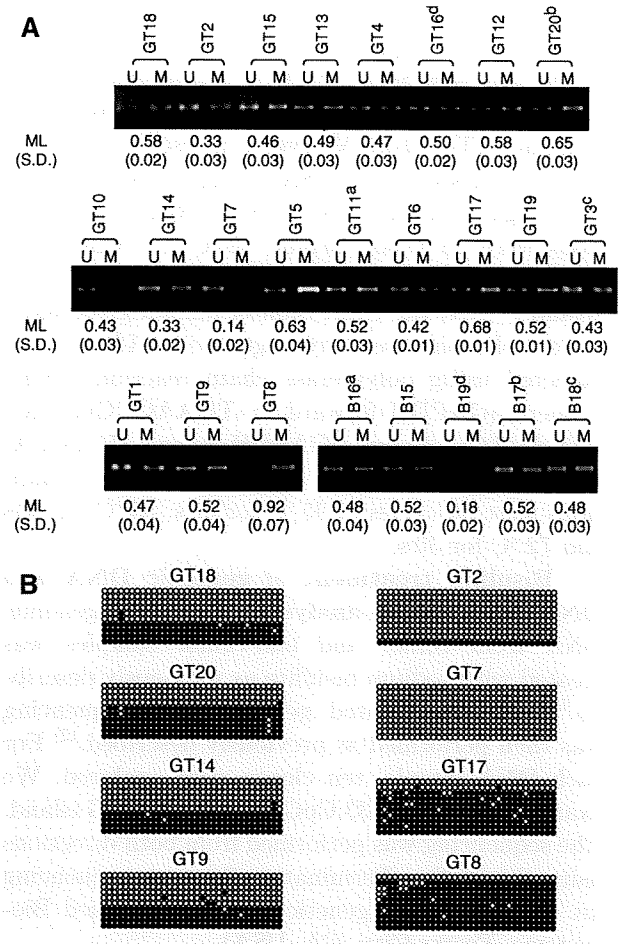

Fig. 2. Methylation of the CpG island localized at the first exon of *PEG3* gene.
(A) Methylation-specific PCR analysis of gliomas (from GT1 to GT20) and non-tumor brain tissues (from B15 to B19). U and M mean PCR products derived from unmethylated and methylated alleles, respectively. Methylation levels (ML) of each sample were calculated as described in materials and methods. Mean of ML and Standard deviation (S.D.) of each sample are indicated under the picture of electrophoresis.
(B) Bisulfite sequencing analysis in the representative tissues. Circles that queue horizontally indicate a clone sequenced. Ten cloned from each samples were sequences. Thirty-three circles indicate CpG sites within the region were analyzed. Open and closed circles indicate unmethylated and methylated cytosines, respectively.

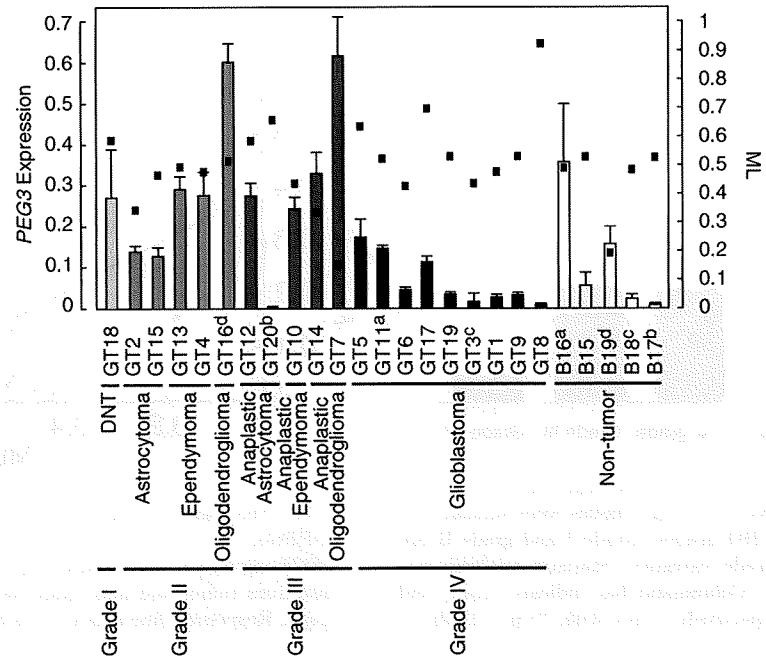

Fig. 3. *PEG3* expression and methylation level in glioma and non-tumor tissues.
Relative expressions of *PEG3* are shown as columns with standard deviation bars. Results of qRT-PCR were standardized by *GAPDH*. Each columns is indicated by the following colors, WHO grade I (□), grade II (▒), grade III (■), grade IV (■) and non-tumor (□) brain tissues. Subtype and WHO grade of glioma were indicated under the sample name. Methylation level (ML) of each sample is shown by closed square.

We attempted to identify differences in methylation between malignancy grades. Average ML values were 0.436 ± 0.144, 0.472 ± 0.080, 0.423 ± 0.202 and 0.568 ± 0.156 in the non-tumor and low-grade, grade III, and grade IV glioma brain tissues, respectively. The ML and tumor grade were statistically unrelated.

To clarify difference of methylation status between tumor and non-tumor, we investigated MLs in tissues from 4 patients who provided both tumor and non-tumor samples. MLs of tumor tissues were higher in samples GT16 ($ML = 0.50$, $P = 0.0000162$) and GT20 ($ML = 0.65$, $P = 0.00701$) than B19 ($ML = 0.18$) and B17 ($ML = 0.52$), respectively. However, there were no significant differences in MLs in samples GT11 ($ML = 0.52$, $P = 0.265$) and GT3 ($ML = 0.43$, $P = 0.145$) compared to B16 ($ML = 0.48$) and B18 ($ML = 0.48$), respectively.

Monoallelic expression of *PEG3* in glioma. Hypomethylation of the CpG island suggests the possibility of biallelic expression of *PEG3*, which indicates deregulation of imprinting. To investigate the allelic pattern of *PEG3* expression, we performed an imprinting test of glioma and non-tumor brain tissues by RT-PCR and direct sequencing of the PCR product. Almost all tissues except sample GT3 verified PCR products. We found, however, monoallelic *PEG3* expression in eight out of nine gliomas and all four non-tumor brain tissues (Table 1).

***PEG3* gene expression.** To determine the *PEG3* expression level, we performed a qRT-PCR assay. After three sets of experiments, average values and SDs of each tissue were calculated (Fig. 3). We found lower expression in six (GT6, GT19, GT3, GT1, GT9 and GT8) out of nine glioblastomas compared with the average value of non-tumor brain tissues. Relatively higher expression of *PEG3* was also found in two oligodendrogliomas (GT16 and GT7) but not in grade II astrocytomas or ependymomas. The average values of *PEG3* expression were 0.124 ± 0.150, 0.285 ± 0.172, 0.294 ± 0.221, and 0.065 ± 0.061 in non-tumor and low-grade, grade III and grade IV glioma brain tissues, respectively. We found significant

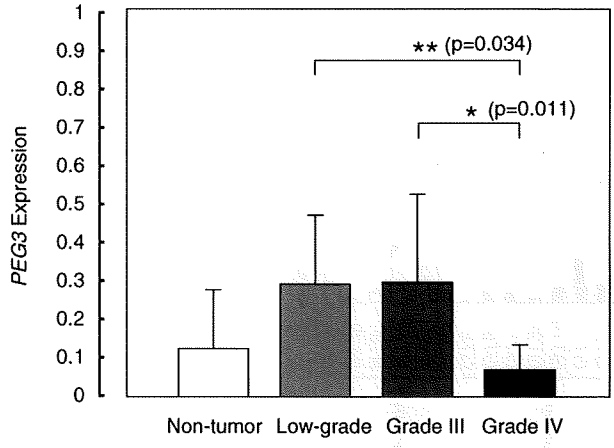

Fig. 4. *PEG3* expression and the grade of glioma.
Twenty gliomas and five non-tumor tissues were summarized into four groups by WHO grades. Grade I and grade II are included in the low-grade category. Statistic analysis was examined by ANOVA. Columnand bar indicate mean, and standard deviation, respectively. *; $p < 0.05$, **; $p < 0.005$.

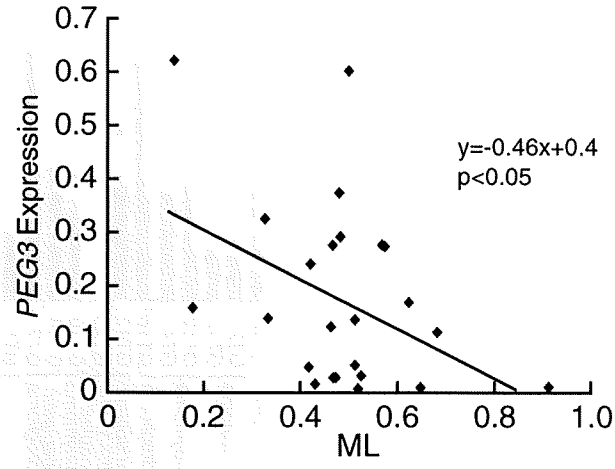

Fig. 5. The regression analysis of expression and methylation of *PEG3*.
PEG3 expression were plotted against methylation level. All data from tumor and non-tumor samples were plotted in the graph. Regression line was $y = -0.46x + 0.4$, $p < 0.05$.

lower gene expression in grade IV than in low-grade and grade III tumors by ANOVA analysis (Fig. 4). Neither low-grade ($p = 0.135$), grade III ($p = 0.193$), nor grade IV ($p = 0.313$) glioma had the significant differences compared with non-tumor tissues.

Negative correlation between *PEG3* expression and ML. In glioma tissues showing hypomethylation (GT7 and GT14), *PEG3* expression was high. In glioma tissues showing hypermethylation (GT8 and GT17), contrastingly, *PEG3* expression was low. We also found a trend toward a negative correlation between *PEG3* expression and ML (Fig. 3). To confirm this trend, we performed a regression analysis and found a weak negative correlation ($r = -0.407$, $P < 0.05$) (Fig. 5). Our result provided evidence that *PEG3* expression is regulated by methylation of the CpG island.

It is thought that the age and sex of patients are associated with particular types of gliomas.[16] To investigate whether there is any association between the age or sex of patients and *PEG3* gene expression, we performed another regression analysis. No significant correlation was found (data not shown).

Discussion

In our previous report,[11] downregulation of *PEG3* was found in glioma cell lines. However, it was not clear whether a similar downregulation occurs in glioma tissues and whether there is any relationship between gene expression and tumor subtype or grade. In the current study, six out of nine glioblastomas showed lower mRNA levels than mean levels of non-tumor brain tissues (Fig. 3). The downregulation was statistically confirmed in grade IV glioblastomas, compared with low-grade and grade III gliomas (Fig. 4). These results suggest that *PEG3* downregulation is associated with glioblastoma. Downregulation of *PEG3* has been found in ovarian cancer cell lines and in nonendometrial and endometrial cancers and the promoter was hypermethylated.[17)–19)] Thus, *PEG3* might play an important role in various types of cancer.

MLs of grade IV glioblastomas seem slightly higher than those in non-tumor brain tissues. However, there was no significance in static test. Nevertheless, hypermethylation of the CpG island was previously reported in glioma cells. Moreover, regression study demonstrated *PEG3* expression has negative correlation with the methylation of the CpG island (Fig. 5). It is possible that the significance of this regression due to higher expression of *PEG3* gene in oligodendroglioma. Although further study might be necessary to careful elucidation of this relationship between methylation and expression, our results indicated that *PEG3* downregulation is due to methylation of the CpG island.

Moreover, ML in a tumor GT20 was higher than matched non-tumor sample B17. The methylation is possibly increased in tumorigenesis.

Loss of imprinting, biallelic expression, and epigenetic silencing of an imprinted gene are frequently observed in various types of cancer — for example, biallelic expression of insulin-like growth factor 2 and epigenetic silencing of cyclin-dependent kinase inhibitor 1C.[20),21)] Previously, we reported the gene suppression of *PEG3* in glioma cell lines.[11)] Biallelic *PEG3* expression has also been reported in two choriocarcinoma cell lines.[19)] Furthermore, the mouse embryonic fibroblasts derived from imprint-free embryonic stem cells, which have loss of imprinting of multiple imprinted genes, including biallelic *PEG3* expression, formed tumors in the immunodeficient mouse model.[22)] These results suggest that both loss of imprinting and epigenetic silencing of *PEG3* are involved in tumorigenesis. We confirmed the monoallelic expression in eight out of nine informative cases, which suggests that genomic imprinting of *PEG3* is strongly sustained in the brain and is not disrupted in glioma.

Interestingly, we found the highest *PEG3* expression in one grade II and one grade III oligodendroglioma each. Recently, delta-like 1 and *PEG10* gene expression were reported to be upregulated in hepatocellular carcinoma and B cell chronic lymphocytic leukemia, respectively.[23),24)] Additionally, ectopic c-Myc oncogene has been shown to induce *H19* gene expression without affecting its imprinted status in breast epithelial cells.[25)] These implied upregulation of imprinted genes associate with tumor. However, loss of heterozygosity (LOH) of 19q has been frequently observed in oligodendrogliomas, and alterations in parental-origin specific copy number might also affect *PEG3* expression levels.[26)] Furthermore, there has been another report that *PEG3* silencing is associated with oligodendroglioma.[10)] These findings suggest the possibility that both upregulation and downregulation of *PEG3* are involved in tumorigenesis.

Our study had several limitations. We detected wide variations in MLs and *PEG3* expression not only in tumor but also in non-tumor brain tissues. *PEG3* expression levels differed by more than 52-fold between control samples B16 and B17. In contrast, hypomethylation of the CpG island was observed in sample B19 (Fig. 3). These results may due to cell type and/or tissue-specific DNA methylation and epigenetic heterogeneity in the brain tissues among individuals. Furthermore, our non-tumor brain tissue samples may not have been appropriate as normal controls, given that they were obtained adjacent to tumor tissue. Low ML of B19 might be due to LOH of methylated allele. In further study, LOH analysis might be necessary to evaluate relationship between methylation level and allele copy number. Cells of tumor tissues may be heterogeneous, causing the gene to be variably expressed. It will be necessary to determine whether our observations are due to tumorigenesis in the peritumoral region or to natural variations in expression levels.

In our methylation analysis, a number of sample demonstrated normal range, thus its relationship with tumor grade was not clear. However, we observed a negative correlation between *PEG3* expression and the ML (Fig. 5). This indicates the possibility that *PEG3* gene expression is regulated by methylation of the CpG island, as previously reported.[11)] Silencing of the active *PEG3* allele could be caused by multiple factors. Kim *et al.*[27)] reported that Gli-type transcription factor YY-1 binding motifs were localized at the first intron of *PEG3* gene and differentially methylated between two parental alleles in vivo. However, an YY-1–deficient mouse model using shRNA exhibited increased *PEG3* transcripts without alterations in promoter methylation or histone tail methylation.[28)] Furthermore, we found no significant difference in methylation on these motifs in glioma tissues (data not shown). More recently, macroH2A, a variant form of core histone H2A was reported to be deposited on the silencing allele at several imprinting control regions containing *PEG3*.[29)] However, *in vivo* knockdown of macroH2A showed not hypomethylation of *PEG3* but hypermethylation.[30)] Additionally, Lu *et al.*[31)] reported that the cyclophilin A gene protects parental *PEG3* against DNA hypermethylation and tri-methylation of histone H3 lysine 9 in mice. *ITUP1*, which we previously isolated,[12)] might be associated with regulation of 19q13.4 imprinted gene cluster. *PEG3* regulation is complex, and the disruption of these mechanisms might be involved in tumorigenesis.

In conclusion, we found that the deregulation of *PEG3* is associated with specific subtypes of

glioma. However, it will be necessary to investigate this association in a larger cohort by narrow analysis and to determine other epigenetic mechanisms for the regulation of *PEG3* gene expression in glioma. More recently, it was reported that downregulation of *ARHI*, which is an imprinted gene with tumor suppressor activity, was correlated with *PEG3* downregulation in ovarian cancer by using pyrosequencing.[32] This finding suggested coordinate downregulation of imprinted tumor suppressor genes might be associated with tumorigenesis. It is necessary to analyze expression of multiple imprinted genes and the association in glioma.

Acknowledgement

S.O. was supported by Japan Society for the Promotion of Science. The research was supported in part by grants from the Scientific Fund of the Ministry of Education, Culture, Sports, Science and Technology of Japan and the Ministry of Health, Labor and Welfare of Japan.

References

1) Kim, J., Ashworth, L., Branscomb, E. and Stubbs, L. (1997) The human homolog of a mouse-imprinted gene, *Peg3*, maps to a zinc finger gene-rich region of human chromosome 19q13.4. Genome Res. **7**, 532–540.
2) Relaix, F., Wei, X.J., Wu, X. and Sassoon, D.A. (1997) *Peg3/Pw1* is an imprinted gene involved in the TNF-NFκB signal transduction pathway. Nat. Genet. **18**, 287–291.
3) Deng, Y. and Wu, X. (2000) Peg3/Pw1 promotes p53-mediated apoptosis by inducing Bax translocation from cytosol to mitochondria. Proc. Natl. Acad. Sci. USA **97**, 12050–12055.
4) Johnson, M.D., Wu, X., Aithmitti, N. and Morrison, R.S. (2002) Peg3/Pw1 is a mediator between p53 and Bax in DNA damage-induced neuronal death. J. Biol. Chem. **277**, 23000–23007.
5) Yamaguchi, A., Taniguchi, M., Hori, O., Ogawa, S., Tojo, N., Matsuoka, N. *et al.* (2002) Peg3/Pw1 is involved in p53-mediated cell death pathway in brain ischemia/hypoxia. J. Biol. Chem. **277**, 623–629.
6) Kuroiwa, Y., Kaneko-Ishino, T., Kagitani, F., Kohda, T., Li, L.L., Tada, M. *et al.* (1996) *Peg3* imprinted gene on proximal chromosome 7 encodes for a zinc finger protein. Nat. Genet. **12**, 186–190.
7) Li, L.L., Keverne, E.B., Aparicio, S.A., Ishino, F., Barton, S.C. and Surani, M.A. (1999) Regulation of maternal behavior and offspring growth by paternally expressed *Peg3*. Science **284**, 330–333.
8) Szeto, I.Y.Y., Barton, S.C., Keverne, E.B. and Surani, M.A. (2004) Analysis of imprinted murine *Peg3* locus in transgenic mice. Mamm. Genome **15**, 284–295.
9) Curley, J.P., Pinnock, S.B., Dickson, S.L., Thresher, R., Miyoshi, N., Surani, M.A. *et al.* (2005) Increased body fat in mice with a targeted mutation of the paternally expressed imprinted gene *Peg3*. FASEB J. **19**, 1302–1304.
10) Kohda, T., Asai, A., Kuroiwa, Y., Kobayashi, S., Aisaka, K., Nagashima, G. *et al.* (2001) Tumour suppressor activity of human imprinted gene *PEG3* in a glioma cell line. Genes Cells **6**, 237–247.
11) Maegawa, S., Yoshioka, H., Itaba, N., Kubota, N., Nishihara, S., Shirayoshi, Y. *et al.* (2001) Epigenetic silencing of *PEG3* gene expression in human glioma cell lines. Mol. Carcinog. **31**, 1–9.
12) Maegawa, S., Itaba, N., Otsuka, S., Kamitani, H., Watanabe, T., Tahimic, C.G. *et al.* (2004) Coordinate downregulation of a novel imprinted transcript *ITUP1* with *PEG3* in glioma cell lines. DNA Res. **11**, 37–49.
13) Kleihues, P. and Cavenee, K. (eds.) (2000) WHO Classificaton of Tumors: Pathology and Genetics of Tumours of the Nervous System. IARC Press, France.
14) Clark, S.J., Harrison, J., Paul, C.L. and Frommer, M. (1994) High sensitivity mapping of methylated cytosines. Nucleic Acids Res. **22**, 2990–2997.
15) Umbricht, C.B., Evron, E., Gabrielson, E., Ferguson, A., Marks, J. and Sukumar, S. (2001) Hypermethylation of 14-3-3s (stratifin) is an early event in breast cancer. Oncogene **20**, 3348–3353.
16) Margaret, W., Yuriko, M., Terri, C., Melissa, B. and Mitchel, S.B. (2002) Epidemiology of primary brain tumors: Current concepts and review of the literature. Neuro-Oncology **4**, 278–299.
17) Shridhar, V., Sen, A., Chien, J., Staub, J., Avula, R., Kovats, S. *et al.* (2002) Identification of underexpressed genes in early- and late-stage primary ovarian tumors by suppression subtraction hybridization. Cancer Res. **62**, 262–270.
18) Risinger, J.I., Maxwell, G.L., Chandramouli, G.V., Jazaeri, A., Aprelikova, O., Patterson, T. *et al.* (2003) Microarray analysis reveals distinct gene expression profiles among different histologic types of endometrial cancer. Cancer Res. **63**, 6–11.
19) Dowdy, S.C., Gostout, B.S., Shridhar, V., Wu, X., Smith, D.I., Podratz, K.C. *et al.* (2005) Biallelic methylation and silencing of paternally expressed gene 3 (PEG3) in gynecologic cancer cell lines. Gynecol. Oncol. **99**, 126–134.
20) Robertson, K.D. (2005) DNA methylation and human disease. Nat. Rev. Genet. **6**, 597–610.
21) Soejima, H., Nakagawachi, T., Zhao, W., Higashimoto, K., Urano, T., Matsukura, S. *et al.* (2004) Silencing of imprinted *CDKN1C* gene expression is associated with loss of CpG and histone H3 lysine 9 methylation at DMR-

LIT1 in esophageal cancer. Oncogene **23**, 4380–4388.
22) Holm, T.M., Jackson-Grusby, L., Brambrink, T., Yamada, Y., Rideout, W.M. 3rd and Jaenisch, R. (2005) Global loss of imprinting leads to widespread tumorigenesis in adult mice. Cancer Cell **8**, 275–285.
23) Huang, J., Zhang, X., Zhang, M., Zhu, J.D., Zhang, Y.L., Lin, Y. *et al.* (2007) Up-regulation of *DLK1* as an imprinted gene could contribute to human hepatocellular carcinoma. Carcinogenesis **28**, 1094–1103.
24) Kainz, B., Shehata, M., Bilban, M., Kienle, D., Heintel, D., Krömer-Holzinger, E. *et al.* (2007) Overexpression of the paternally expressed gene 10 (PEG10) from the imprinted locus on chromosome 7q21 in high-risk B-cell chronic lymphocytic leukemia. Int. J. Cancer **121**, 1984–1993.
25) Barsyte-Lovejoy, D., Lau, S.K., Boutros, P.C., Khosravi, F., Jurisica, I., Andrulis, I.L. *et al.* (2006) The c-Myc oncogene directly induces the H19 noncoding RNA by allele-specific binding to potentiate tumorigenesis. Cancer Res. **66**, 5330–5337.
26) Trouillard, O., Aguirre-Cruz, L., Hoang-Xuan, K., Marie, Y., Delattre, J.Y. and Sanson, M. (2004) Parental 19q loss and *PEG3* expression in oligodendrogliomas. Cancer Genet. Cytogenet. **151**, 182–183.
27) Kim, J., Kollhoff, A., Bergmann, A. and Stubbs, L. (2003) Methylation-sensitive binding of transcription factor YY1 to an insulator sequence within the paternally expressed imprinted gene, *Peg3*. Hum. Mol. Genet. **12**, 233–245.
28) Kim, J. and Kim, J.D. (2008) *In vivo* YY1 knockdown effects on genomic imprinting. Hum. Mol. Genet. **17**, 391–401.
29) Choo, J.H., Kim, J.D., Chung, J.H., Stubbs, L. and Kim, J. (2006) Allele-specific deposition of macroH2A1 in imprinting control regions. Hum. Mol. Genet. **15**, 717–724.
30) Choo, J.H., Kim, J.D. and Kim, J. (2007) MacroH2A1 knockdown effects on the *Peg3* imprinted domain. BMC Genomics **8**, 479.
31) Lu, Y.C., Song, J., Cho, H.Y., Fan, G., Yokoyama, K.K. and Chiu, R. (2006) Cyclophilin - A protects *Peg3* from hypermethylation and inactive histone modification. J. Biol. Chem. **281**, 39081–39087.
32) Feng, W., Marquez, R.T., Lu, Z., Liu, J., Lu, K., Issa, J.P. *et al.* (2008) Imprinted tumor suppressor genes *ARHI* and *PEG3* are the most frequently down-regulated in human ovarian cancers by loss of heterozygosity and promoter methylation. Cancer **112**, 1489–1502.

(Received Nov. 11, 2008; accepted Mar. 4, 2009)

Molecular Genetics and Metabolism 98 (2009) 393–399

Contents lists available at ScienceDirect

Molecular Genetics and Metabolism

journal homepage: www.elsevier.com/locate/ymgme

Inhibition of autophagosome formation restores mitochondrial function in mucolipidosis II and III skin fibroblasts

Takanobu Otomo [a,1], Katsumi Higaki [b,1], Eiji Nanba [b], Keiichi Ozono [a], Norio Sakai [a,*]

[a] Department of Pediatrics (D-5), Osaka University Graduate School of Medicine, 2-2 Yamadaoka, Suita, Osaka 565-0871, Japan
[b] Division of Functional Genomics, Research Center for Bioscience and Technology, Tottori University, 86 Nishi-cho, Yonago 683-8503, Japan

ARTICLE INFO

Article history:
Received 1 July 2009
Accepted 1 July 2009
Available online 7 July 2009

Keywords:
Mucolipidosis II and III
Inclusion body
Autophagy
Mitochondrial impairment

ABSTRACT

Mucolipidosis II and III are progressive lysosomal storage disorders caused by a deficiency of *N*-acetylglucosamine-1-phosphotransferase, leading to massive accumulation of undigested substrates in lysosomes (inclusion bodies) in skin fibroblast. In this study, we demonstrated accumulation of autolysosomes and increased levels of p62 and ubiquitin proteins in cultured fibroblasts. These autophagic elevations were milder in mucolipidosis III compared with mucolipidosis II. Mitochondrial structure was fragmented and activity was impaired in the affected cells, and 3-methyladenine, an inhibitor of autophagosome formation, restored these. These results show for the first time autophagic and mitochondrial dysfunctions in this disorder.

1. Introduction

Mucolipidosis (ML)[2] II and III are autosomal recessive diseases caused by a deficiency of UDP-*N*-acetylglucosamine:lysosomal enzyme *N*-acetylglucosamine-1-phosphotransferase (GlcNAc-phosphotransferase) and is characterized clinically by developmental delay and dysostosis multiplex, which overlap partially with mucopolysaccharidoses [1]. GlcNAc-phosphotransferase is composed of six subunits $\alpha_2\beta_2\gamma_2$. The α and β subunits are encoded by a single gene *GNPTAB* and the γ subunit by *GNPTG* [2,3]. Mutations in *GNPTAB* cause both severe type ML (ML II alpha/beta, MIM #252500) and attenuated type ML (ML III alpha/beta, MIM #252600), and mutations in *GNPTG* cause only attenuated type ML (ML III gamma, MIM #252605) [3–6]. GlcNAc-phosphotransferase acts in the first step of synthesizing the mannose 6 phosphate (M6P) recognition marker on lysosomal enzyme proteins, which is recognized by M6P receptor for targeting to the lysosome [7]. In ML patients, lysosomal enzymes lack M6P residues and are hypersecreted into the extracellular space and body fluids instead of being targeted to the lysosome. One of the most characteristic features of these diseases is the presence of numerous phase-dense "inclusion bodies" in patients' skin fibroblasts, which are thought to be lysosomes filled with undigested compounds. However, their contribution to the pathology of ML II and III are still unclear.

Macroautophagy (hereafter referred to as autophagy) is a lysosomal degradation pathway that is essential for cellular survival [8]. Autophagy not only provides nutrients during fasting but also maintains inner cellular routine turnover by degrading misfolded proteins and damaged organelles such as mitochondria, peroxisomes and endoplasmic reticulum. Recent reports show abnormal lysosomal storage blocks the autophagy pathway and the ubiquitin pathway in lysosomal storage diseases [9,10], but the connection between inclusion body formation and the autophagy pathway in ML II and III cells is not known. In this study we found accumulation of autolysosomes followed by mitochondrial dysfunction in ML fibroblasts, and impaired mitochondrial function was restored by 3-MA, an inhibitor of autophagosome formation. Moreover, these autophagic aberrations indicated some correlation with the severity of clinical phenotypes.

2. Materials and methods

2.1. Cell culture

Human skin fibroblasts from a normal control and ML II, ML III patients were cultured in Dulbecco's modified Eagle's medium (DMEM) supplemented with 10% fetal bovine serum (FBS) and Antibiotic–Antimycotic (GIBCO, Grand Island, NY, USA) with the informed consent of patients. ML II skin fibroblasts had homozygous mutation of c.3565C > T (p.R1189X) in the *GNPTAB* gene,

* Corresponding author. Tel.: +81 6 6879 3932; fax: +81 6 6879 3939.
E-mail address: norio@ped.med.osaka-u.ac.jp (N. Sakai).

[1] These authors contributed equally to this work.

[2] *Abbreviations used:* ML, mucolipidosis; GlcNAc-phosphotransferase, UDP-*N*-acetylglucosamine:lysosomal enzyme *N*-acetylglucosamine-1-phosphotransferase; M6P, mannose 6 phosphate; LC3, microtubule-associated protein 1 light chain 3; Lamp-2, lysosomal associated membrane protein-2; 3-MA, 3-methyladenine; DMEM, Dulbecco's modified Eagle's medium; PBS, phosphate-buffered saline; BSA, bovine serum albumin; Ub, ubiquitin.

1096-7192/$ - see front matter © 2009 Elsevier Inc. All rights reserved.
doi:10.1016/j.ymgme.2009.07.002

and ML III had compound heterozygote mutations of c.1120T > C (p.F374L) and c.3565C > T (p.R1189X) in the *GNPTAB* gene. These mutations are common in Japanese patients, as reported in the previous paper [11].

2.2. Antibodies and reagents

Polyclonal anti-LC3 (PD014), polyclonal anti-p62/SQSTM1 (PM045) (MBL Co. Ltd., Nagoya, Japan), polyclonal anti-beclin-1 (H-300), monoclonal anti-Ub (P4D1), polyclonal anti-β-tubulin (H-235), monoclonal anti-Lamp-2 (H4B4), polyclonal anti-cathepsin B (S-12), polyclonal anti-cathepsin D (H-75) (Santa Cruz Biotech. Inc., Santa Cruz, CA, USA), monoclonal anti-Tim23 (611223) (BD Biosciences, San Jose, CA, USA), monodansylcadaverine (MDC), and 3-methyladenine (3-MA) (Sigma–Aldrich, St. Louis, MO, USA) were purchased.

2.3. Protein extraction and immunoblotting

Protein extraction from cultured human skin fibroblasts and immunoblotting was performed as described previously [12]. Briefly, equal amounts of proteins (10–20 μg) were electrophoresed in acrylamide gels and subjected to immunoblotting. After incubation with HRP-conjugated secondary antibodies, the membranes were developed using ECL plus reagent (GE Healthcare) and images were captured using X-ray film (RX-U; Fujifilm Co., Tokyo, Japan).

2.4. Fluorescence staining and microscopy

Immunofluorescence staining was performed as described previously [12]. Briefly, cells on coverslips were incubated with primary antibodies against LC3 (1:100), Lamp-2 (1:100), beclin-1 (1:100), ubiquitin (1:100), p62 (1:500), or Tim23 (1:100) for 60 min at room temperature (RT) or 4 °C overnight, and bound antibodies were detected using Alexa Fluor-conjugated secondary antibodies (1:2000 dilution with 0.1% BSA in PBS) for 60 min at RT. For autophagic vacuole labeling, cells were incubated with 50 μM MDC for 10 min at 37 °C. For lysosome staining, cells were incubated with LysoTracker Red DND-99 (100 nM, Molecular Probes Inc., Eugene, OR, USA) for 60 min at 37 °C. For mitochondria staining, cells were incubated with MitoTracker Red CMXRos (100 nM, Molecular Probes Inc.) or JC-1 (3 μM, Molecular Probes Inc.) for 20 min at 37 °C. All fluorescence images were acquired using a fluorescence microscope (Leica DMIRE2; Leica Microsystems, Wetzlar, Germany) or a confocal laser scan microscopy system (Leica TCS SP-2; Leica Microsystems).

2.5. Cathepsin B enzyme activity

The activity of cathepsin B was measured using Magic Red Cathepsin B detection kit (Immunochemistry Tech. LLC, Bloomington, MN, USA). Briefly, cells were prepared on the 96-well cultured plate and incubated with fluorogenic substrate for cathepsin B ($MR-(RR)_2$). Fluorescence was measured using a fluorescence mul-

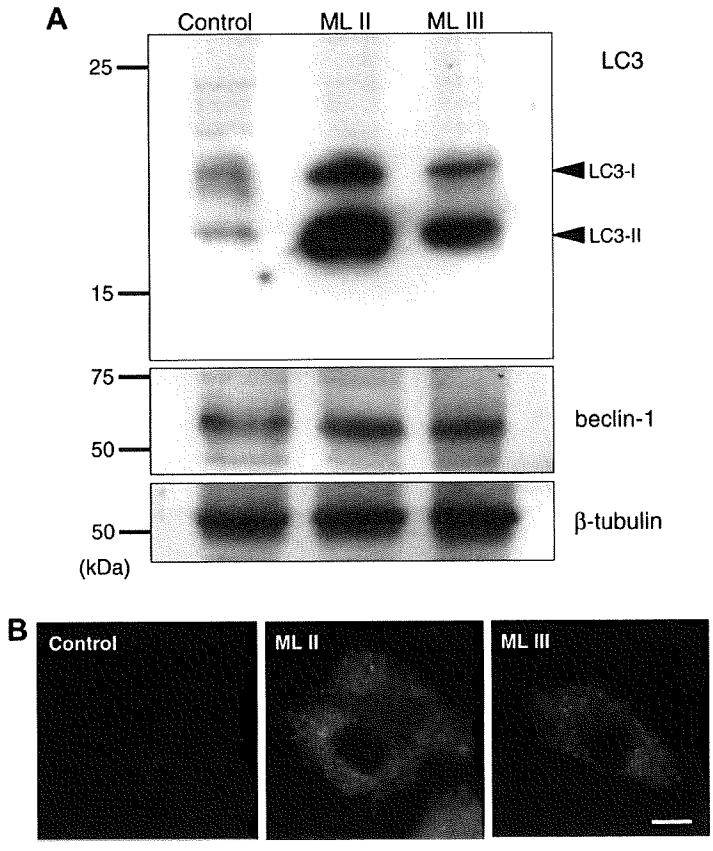

Fig. 1. Elevation of autophagosome formation in ML fibroblasts. (A) Anti-LC3 and beclin-1 immunoblotting of lysates from control, ML II and ML III skin fibroblasts. Densitometric image analysis shows 1.479, 13.862 and 9.672 for LC3-II/LC3-I (average intensities of at least two independent examinations), and 1.028, 0.938 and 0.954 for beclin-1/β-tubulin (average intensities of at least three independent examinations), in control, ML II and ML III, respectively. (B) MDC staining. (C and D) Immunofluorescence of cellular distribution of LC3 with LysoTracker (C) and LC3 with Lamp-2 (D). Bar = 10 μm.

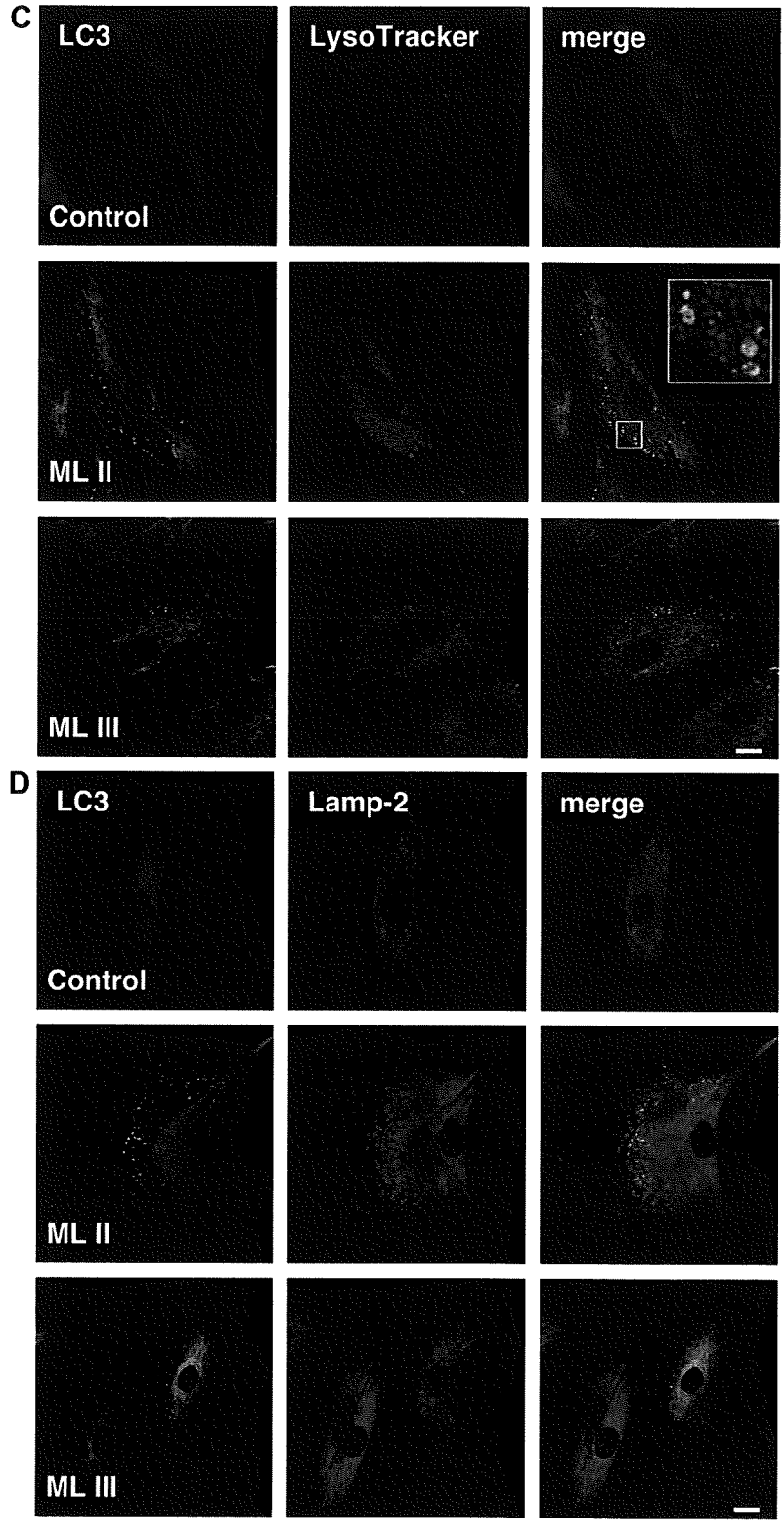

Fig. 1 (*continued*)